

Molecular Rydberg transitions. Multichannel approaches to electronic states: CH₃I

J. A. Dagata, G. L. Findley, and S. P. McGlynn

Choppin Chemical Laboratories, Louisiana State University, Baton Rouge, Louisiana 70803

J. -P. Connerade

Physics Department, Imperial College of Science and Technology, Prince Consort Road, London SW7 2BZ England

M. A. Baig

Physikalisches Institut, Universität Bonn, Nussallee 12, 5300 Bonn 1, West Germany

(Received 22 June 1981)

A multichannel quantum-defect theoretic (MQDT) analysis of the high-resolution vacuum-ultraviolet spectrum of CH₃I in the energetic region below the first ionization limit is presented. The analysis is based upon, and substantiates *a posteriori*, quantum-defect analogies between Xe and CH₃I: that is, only purely electronic molecular channels are allowed to interact. A new *d* series converging on the first ionization limit is assigned as a result of the MQDT analysis.

I. INTRODUCTION

In the simplest approximation, a Rydberg (R) transition in a neutral atom or molecule is defined as a member of a series of transitions which obey the Rydberg equation

$$E_{j\alpha} = I - R/v_{j\alpha}^2, \quad (1)$$

where $E_{j\alpha}$ is the energy of that spectral feature which is thought to be the j th member of the α th R series converging on the ionization limit I , R is the Rydberg constant, and $v_{j\alpha}$ is the effective quantum number.

The classical method of assignment of an R series involves finding a "best fit" of experimental data to Eq. (1). This procedure, however, presupposes that the spectrum under study exhibits high resolution over the entire region from the lowest-energy R transition to the corresponding ionization limit, and that there is little perturbation of one R series by another. For molecules, these criteria are infrequently satisfied.

Deeper insight into Eq. (1) is found by making contact with the quantum defect theory (QDT) of Seaton¹ in which

$$v_{j\alpha} = n_j - \mu_\alpha, \quad \delta_\alpha = \pi\mu_\alpha, \quad (2)$$

where n_j is a positive integer (indeed, when $\mu_\alpha = 0$, $n_j \equiv n$, the *aufbau* quantum number), μ_α is the quantum defect of the α th R series, and δ_α is the

phase shift of a scattered electron associated with the α th R series. One immediate advantage of the QDT approach is that bound states and scattering states are treated on an equal footing as members of a "channel": All states, both bound and scattering, which are associated with the α th R series serve to define the α th channel. QDT, in general, is concerned with the description of channel structures and interchannel interactions. If interchannel interactions are assumed to be negligible, single-channel QDT (SQDT) results; multichannel QDT (MQDT) takes these perturbations into account.

In SQDT, orbital angular momentum of the optical electron is conserved and, hence, $\alpha \equiv l$. In N -electron atoms, however, additional channels arise because of the multiplicity of core states — an effect resulting primarily from exchange and spin-orbit coupling interactions. A more correct rendering of Eq. (1), therefore, requires an index labeling the ionization potential:

$$E_{i,jl} = I_i - R/v_{i,jl}^2. \quad (3)$$

The situation is even more complicated in molecules, where the number of possible channels further increases because of symmetry lowering and rotational-vibrational effects.²

In MQDT, on the other hand, orbital angular momentum of the optical electron is not conserved. This leads to a mixing of channels having the same *total* angular momentum and this mixing, in turn,

destroys the "goodness" of l . In more arcane phraseology, the l basis does not diagonalize the S matrix in the presence of interchannel interactions. MQDT, however, provides an *ansatz* for constructing a diagonalizing basis.

The purpose of this paper is to provide an MQDT analysis of the vacuum-ultraviolet spectrum of CH_3I in the region below the first ionization limit. A prime motivation for this work was our earlier³ SQDT analysis of CH_3I and HI treated as analogs of Xe . In that paper³ we adopted the attitude that the R states of CH_3I and HI could be viewed as slightly perturbed analogs of the R states of Xe — an attitude which led ultimately to an ability to estimate the range and effectiveness of one-electron molecular potentials for these molecules. Our present work is, in part, an extension of these attitudes. This extension transcends our earlier approach, however, in several important ways.

- (a) We have validated the use of MQDT for purely electronic *molecular* channels.
- (b) We have further substantiated our approach of treating CH_3I as perturbed Xe .
- (c) We have assigned a new d series in CH_3I , which cannot be assigned in the absence of an MQDT analysis.

Two preconditions for this work immediately obtain:

(a) MQDT analysis depends crucially upon high-resolution data, and such data (0.003 Å resolution, obtained at the University of Bonn synchrotron source) have only recently become available for CH_3I .⁴ Indeed, our success in the present paper has induced us to undertake an extensive high-resolution survey of the vuv spectra of the other methyl halides and the hydrogen halides. The results of this survey will be reported in the near future.

(b) Our treatment of CH_3I , in analogy to Xe , precludes any consideration of rotational and vibrational effects. Thus, we formally ignore many additional molecular channels which, *a priori*, may or may not give rise to significant interactions. Two comments are trenchant in justification of this approximation: (i) Our ability to provide a consistent MQDT analysis of the CH_3I vuv data provides *a posteriori* support for the validity of our neglect of rotational/vibrational interactions; and (ii) even at high resolution, the spectrum of CH_3I shows no rotational structure.

Section II of this paper provides a very brief sketch of MQDT and, in particular, describes the

procedure of the Lu-Fano graphical analysis⁵⁻⁷ with reference to Xe . Our CH_3I results are presented in Sec. III and a discussion of these results is given in Sec. IV.

II. MQDT

A. Molecular potentials

QDT starts from a one-electron, radial Schrödinger equation having a potential, in the atomic case, of the form

$$V(r) = V_C(r) + V_a(r) \quad , \quad (4)$$

where $V_C(r)$ is the dominant Coulomb potential, while $V_a(r)$ is a short-ranged, residual-atomic potential of finite effective radius. In the molecular case, however, an anisotropic, residual-molecular potential must be added:

$$V(\vec{r}) = V_C(r) + V_a(r) + V_m(\vec{r}) \quad . \quad (5)$$

We have shown previously³ that, in the case of CH_3I , $V_a(r)$ is that appropriate for Xe , and $V_m(\vec{r})$ is short-ranged and confined to regions of the potential interior to the centrifugal barrier. Indeed, for $l \geq 2$, $V_m(\vec{r})$ is essentially ineffective. Since the short-ranged potentials contribute to deviations of the phase shift (or, equivalently, to deviations of the quantum defect) from the hydrogenic norm, one expects that the nature of $V_m(\vec{r})$ will contribute to a decrease in the quantum defect of the "s" channel of CH_3I relative to that of Xe , while the "d" channels of both CH_3I and Xe will be fully comparable. As will be shown below, such is indeed the case. Thus, the above partitioning of the potential is substantiated.

B. Wave functions

Discrete and continuum wave functions for the optical electron are determined by the imposition of appropriate boundary conditions on a linear combination of regular and irregular Coulomb functions. For the discrete case, in a single-channel format, these boundary conditions reduce to

$$\sin\pi(\nu + \mu) = 0 \quad , \quad (6)$$

or, equivalently,

$$\nu \equiv \nu_j = n_j - \mu \quad . \quad (7)$$

Since each single channel i specifies both the ener-

gy and angular momentum of the core and optical electron components, the multichannel (or, close-coupling eigenchannel) α is a superposition of single-channel states having the same total energy and total angular momentum and influenced by the same core conditions (i.e., possessing the same quantum defect). Following Ref. 7, we may write the total wave function Ψ as a superposition of close-coupling wave functions

$$\Psi = \sum_{\alpha} \Psi_{\alpha} A_{\alpha} \quad (8)$$

and, imposing the appropriate boundary conditions for discrete states, we find

$$\sum_{\alpha} U_{i\alpha} \sin[\pi(\nu_i + \mu_{\alpha})] A_{\alpha} = 0 \quad (9)$$

where $U_{i\alpha} \equiv \langle \Psi_i | \Psi_{\alpha} \rangle$ is that unitary transformation which diagonalizes the scattering matrix. Equation (9), of course, is simply the multichannel correspondent of Eq. (6). Equation (9) is processed via the Lu-Fano graphical analysis, as discussed in the following section.

C. Graphical analysis

We adopt Xe as our prototype. The five Rydberg series of Xe, each having total angular momentum $J=1$, which converge on either $^2P_{3/2}$ or $^2P_{1/2}$ core states are presented in Table I. In a multichannel format, however, each discrete energy level must be referenced with respect to *both* ionization limits [$I_1 \equiv I(^2P_{3/2})$, $I_2 \equiv I(^2P_{1/2})$]. Hence,

for each discrete level of excitation energy E , the Rydberg equation becomes⁸

$$E = I_1 - R/\nu_1^2 = I_2 - R/\nu_2^2 \quad (10)$$

which may be rewritten as

$$\nu_2 = \nu_1 [1 + R^{-1}(I_2 - I_1)\nu_1^2]^{-1/2} \quad (11)$$

Equation (11) will be referred to as $\nu_2(\nu_1)$.

Determination of eigenenergies and eigenfunctions for the discrete states requires the solution of the five equations given in Eq. (9). Lu⁷ has presented a substitution which reduces these five equations to a system of two equations in two unknowns and has shown that this system has non-trivial solutions when a certain consistency function $F(\nu_1, \nu_2)$ vanishes identically. [$F(\nu_1, \nu_2)$ is quadratic in the cotangent of the difference in effective quantum numbers ($\nu_2 - \nu_1$), with coefficients which are functions of ν_1 , μ_{α} , and $U_{i\alpha}$]. The discrete energy levels are then given by pairs of effective quantum numbers which satisfy Eq. (11) and $F(\nu_1, \nu_2) = 0$ simultaneously. Solution is by a graphical procedure which is illustrated in Fig. 1 for Xe.

Since $F(\nu_1, \nu_2) = 0$ is quadratic in the cotangent of effective quantum number differences, it may be plotted modulo 1. Hence, on a plot of ν_2 (modulo 1) versus ν_1 (modulo 1), the discrete levels lie on a series of closed curves determined by $F(\nu_1, \nu_2) = 0$. Because of coupling, however, these curves exhibit avoided crossings in regions of strong perturbation and join into a single continuous curve. The final locations of the discrete levels

TABLE I. Dissociation and close-coupling channels for Xe ($J=1$) and CH₃I ($M_J=1$).

Index ^a	Dissociation channels ^b		Close-coupling channels ^b		Index ^a
	(Ω, ω) CH ₃ I ⁺ + e ⁻	(j, j) Xe ⁺ + e ⁻	(L, S) Xe	(Λ, S) CH ₃ I	
i = 1	[² Π _{3/2}]nd _π	[² P _{3/2}]nd _{5/2}	nd(³ D ₁)	nd _π (³ Δ ₁)	2 = α
2	{ [² Π _{3/2}]nd _σ [² Π _{3/2}]nd _δ }	[² P _{3/2}]nd _{3/2}	nd(³ P ₁)	{ nd _σ (³ Π ₁) nd _δ (³ Π ₁) }	1
3	[² Π _{3/2}]ns	[² P _{3/2}]ns _{1/2}	ns(³ P ₁)	ns(³ Π ₁)	4
4	{ [² Π _{1/2}]nd _σ [² Π _{1/2}]nd _π [² Π _{1/2}]nd _δ }	[² P _{1/2}]nd _{3/2}	nd(¹ P ₁)	{ nd _σ (¹ Π ₁) nd _π (³ Σ ₁ [±]) nd _δ (¹ Π ₁) }	3
5	[² Π _{1/2}]ns	[² P _{1/2}]ns _{1/2}	ns(¹ P ₁)	ns(¹ Π ₁)	5

^aListing of channel indices i and α corresponds to that given in Ref. 7.

^bSymmetry labels for CH₃I are primitive C_{∞v}.

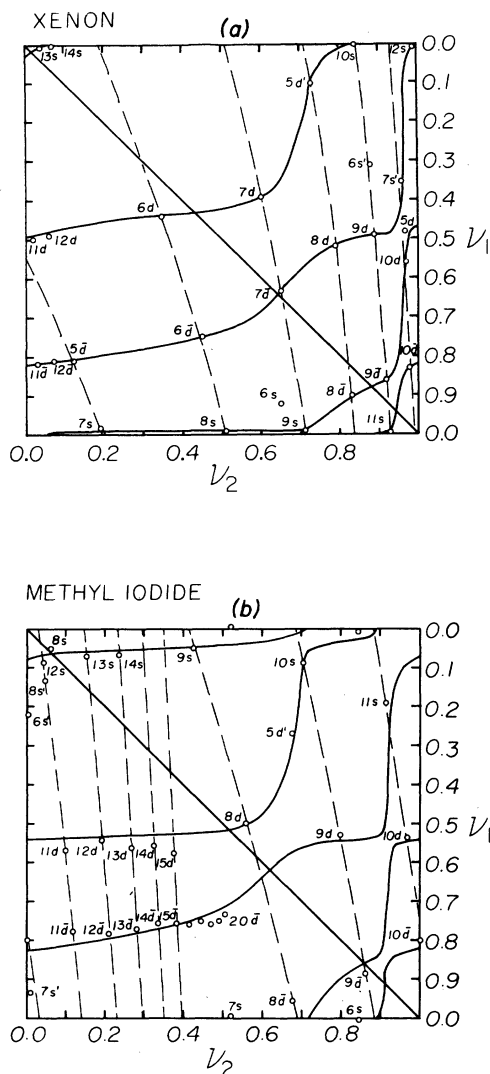


FIG. 1. Lu-Fano plots for the discrete states of Xe (a) and CH_3I (b). The Xe plot is adapted from Ref. 7. ν_1 and ν_2 are effective quantum numbers (modulo 1) defined with respect to the first and second ionization potentials, respectively. The solid, diagonal line is given by $\nu_1 = \nu_2$, the solid curve is the locus of $F(\nu_1, \nu_2) = 0$, and the dashed curve is the function $\nu_2(\nu_1)$. (See text for a description of these curves.) Data point notation are as follows: $d = d_{5/2}(I_1)$, $\bar{d} = d_{3/2}(I_1)$, $s = s_{1/2}(I_1)$; $s' = s_{1/2}(I_2)$; $d' = d_{3/2}(I_2)$.

are given by the intersections of $F(\nu_1, \nu_2) = 0$ with $\nu_2(\nu_1)$. The data-fitting procedure then treats the μ_α and $U_{i\alpha}$ as adjustable parameters. The points of intersection of $F(\nu_1, \nu_2) = 0$ with the diagonal (i.e., $\nu_1 = \nu_2$) determine the eigenquantum defects since, at these points, $\nu_1 = \nu_2 = -\mu_\alpha$ (modulo 1); and the slope of $F(\nu_1, \nu_2) = 0$ at these same points determines the coupling parameters $U_{i\alpha}$. The MQDT

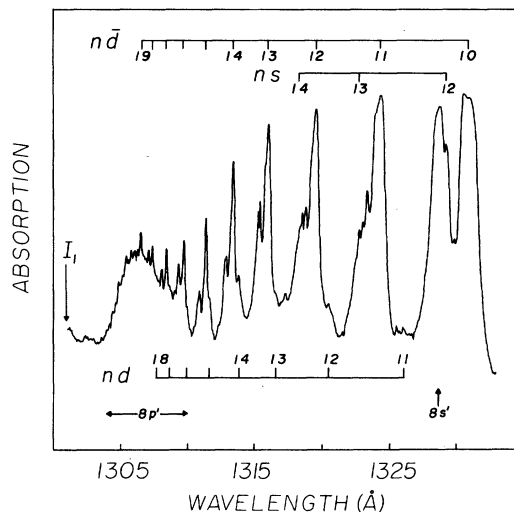


FIG. 2. High-resolution ($0.003\text{-}\text{\AA}$) absorption spectrum of CH_3I in the region $75\,000\text{--}76\,400\text{ cm}^{-1}$. The notation is explained in the caption of Fig. 1. This figure is adapted from Ref. 4.

parameters for Xe, as determined from Fig. 1, are given in Table II.

III. RESULTS: CH_3I

The high-resolution ($0.003\text{-}\text{\AA}$) vuv spectrum of CH_3I in the energy region $75\,000\text{--}76\,400\text{ cm}^{-1}$ is shown in Fig. 2. These data, along with the lower-energy, low-resolution (0.3\AA) assignments of Refs. 3, and 9-11 were used to construct the CH_3I Lu-Fano plot shown in Fig. 1. The fitted MQDT parameters are given in Table II.

Channel symmetries for CH_3I R states ($M_J = 1$) are given in Table I, with the assumption of primitive $C_{\infty v}$ symmetry: That is, we regard CH_3I as being effectively linear—a supposition which we have validated elsewhere.^{3,10,12} In addition, not all formally allowed R series have appreciable intensity: No np series are included in Table I since magnetic circular dichroism analyses¹¹ show these series to be very weak and to disappear after the first few members. Finally, the multiplet splittings of the $nd_{3/2}(I_1)$ and $nd_{3/2}(I_2)$ series are small enough at high energies to be neglected; at low energies, energy-weighted barycenters are appropriate but the multiplet splittings are still small enough to preclude appreciable interactions with other channels.

Our main conclusions are as follows:

(a) MQDT analyses of purely electronic molecular channels are feasible, at least for molecules with highly localized R chromophores.

TABLE II. MQDT parameters^a for Xe^b and CH₃I.

Index	μ_α		$U_{4\alpha}^2$		$U_{5\alpha}^2$	
	Xe	CH ₃ I	Xe	CH ₃ I	Xe	CH ₃ I
$\alpha = 1$	0.57	0.48	0.13	0.16		
2	0.36	0.37	0.48	0.50		
3	0.13	0.14	0.37	0.32		
4	0.05	0.09			0.80	0.90
5	-0.007	-0.065			0.17	0.08

^aCoupling parameters were fitted under the assumption of minimal s/d interaction.

^bXe parameters are taken from Ref. 7.

(b) The similarities between Xe and CH₃I, as evidenced in Fig. 1 and Table II, are most impressive. These similarities clearly indicate the validity of treating CH₃I as a slightly perturbed Xe as far as R structure is concerned.

(c) A new d series, namely $nd_{5/2}(I_1)$, has been located and assigned. It is obvious from Fig. 2 that this series could not have been assigned by conventional techniques in the absence of an MQDT analysis.

(d) The Lu-Fano plot indicates that the low-resolution assignments^{3,9-11} are consistent with the high-resolution assignments and, by and large, probably correct.

IV. DISCUSSION

Given the inherent difficulty in assigning molecular Rydberg states (as evidenced by the paucity of molecular assignments in comparison to atomic assignments), it is crucial to exploit fully our atomic intuition and to transfer it into the molecular realm whenever possible. In this paper we have attempted to use Xe as a model for describing the R structure of CH₃I in an MQDT format. In the end, because of the necessity of some rather heuristic ap-

proximations, one can only say that we have provided a qualitative, albeit powerful, rationalization of CH₃I R series. However, with the extension of this approach to other methyl halides, hydrogen halides, and the associated rare gases,¹³ the limitations of considering purely electronic channel interactions in molecules should become delineated. Nevertheless, the potential power of MQDT to simplify assignment of molecular R states is quite promising.

Finally, we emphasize that we have not discussed the band shapes of the autoionizing states of CH₃I. Such states have, in fact, been demonstrated both in CH₃I (Ref. 3) and CH₃Br (Ref. 14) and have been shown to exhibit a Beutler-Fano^{6,15,16} characteristic. MQDT can be used to calculate these bandshapes but, at present, we defer this result to a later publication.¹³

ACKNOWLEDGMENTS

The work of J.A.D., G.L.F., and S.P.M. was supported by the U.S. Department of Energy. The work of J.P.C. was supported by the UKSRC. The work of M.A.B. was supported by an Alexander von Humboldt fellowship and the DFG.

¹M. J. Seaton, Proc. Phys. Soc. London **88**, 801 (1966); **88**, 815 (1966).

²F. H. Mies, Mol. Phys. **14**, 953 (1980); **14**, 973 (1980).

³H. -t. Wang, W. S. Felps, G. L. Findley, A. R. P. Rau, and S. P. McGlynn, J. Chem. Phys. **67**, 3940 (1977).

⁴M. A. Baig, J. P. Connerade, J. Dagata, and S. P. McGlynn, J. Phys. B **14**, L25 (1981).

⁵K. T. Lu and U. Fano, Phys. Rev. A **2**, 81 (1970).

⁶U. Fano, Phys. Rev. A **2**, 353 (1970).

⁷K. T. Lu, Phys. Rev. A **4**, 579 (1971).

⁸The reader should note that, for convenience, all indexing of effective quantum numbers has been omitted in what follows, except for that necessary to distinguish ionization limits.

⁹W. S. Felps, P. Hochmann, P. Brint, and S. P. McGlynn, J. Mol. Spectrosc. **59**, 355 (1976).

¹⁰J. D. Scott, W. S. Felps, G. L. Findley, and S. P. McGlynn, J. Chem. Phys. **68**, 4678 (1978).

¹¹W. S. Felps and S. P. McGlynn (unpublished).

¹²W. S. Felps, G. L. Findley, and S. P. McGlynn,

Chem. Phys. Lett. (in press).

¹³J. Dagata, G. L. Findley, S. P. McGlynn, J. P. Connerade, and M. A. Baig (unpublished).

¹⁴J. P. Connerade, M. A. Baig, and S. P. McGlynn, J.

Phys. B 14, L67 (1981).

¹⁵H. Beutler, Z. Phys. 93, 177 (1935).

¹⁶U. Fano, Phys. Rev. 124, 1866 (1961).